Preparation of Gd_2O_3 Ultrafine Nanoparticles by Pulse Electrodeposition Followed by Heat-treatment Method

Mustafa Aghazadeh*[1]

[1]*Nuclear Fuel Cycle Research School (NFCRS), Nuclear Science and Technology Research Institute, Tehran.*

ABSTRACT

Gd_2O_3 nanoparticles were prepared by a two–step process; cathodic electrodeposition followed by heat-treatment method. First, $Gd(OH)_3$ nanoparticles was galvanostatically deposited from nitrate bath on the steel substrate by pulse current (PC) mode. The deposition experiments was conducted at a typical on-time and off-time (t_{on}=1ms and t_{off}=1ms) for 60 min. The electrodeposited precursor was then heat-treated at 600 °C for 3h to obtain oxide product (i.e. Gd_2O_3). The morphological and structural analyses confirmed that the gadolinium hydroxynitrate nanoparticles with composition of $[Gd(OH)_{2.5} (NO_3)_{0.5} yH_2O]$ and uniform size about 10 nm have been prepared during pulse cathodic electrodeposition process. Furthermore, mechanism of the gadolinium hydroxynitrate nanoparticles was explained based on the base (OH^-) electrogeneration process on the cathode surface. The morphological observations by SEM and TEM, and structural analyses via XRD and FT-IR revealed that the oxide product is composed of well-dispersed Gd_2O_3 nanoparticles with pure cubic crystalline structure. It was observed that the calcination process has no effect on the morphology of the Gd_2O_3 nanoparticles. Mechanism of oxide formation during heat-treatment step was investigated by DSC-TG analysis and discussed in detail. The results of this work showed that pulse current deposition followed by heat–treatment can be recognized as an easy and facile method for preparation of the Gd_2O_3 fine nanoparticles.

Keywords: *Gd_2O_3; Nanoparticles; Pulse electrodeposition; Heat treatment.*

1. Introduction

Preparation of metal oxides nanoparticles with well-dispersion and defined shapes and sizes, has received considerable attention because of the potential applications of nanoparticles in many different fields like catalysis, sensors, batteries, and solar cells [1,2]. The rare earth oxides as an important engineering materials are used in critical segments of electronic, magnetic, nuclear, optical, and catalytic devices [3,4]. Gadolinium oxide (Gd_2O_3), one of the rare earth oxides, has found use as a high-efficient phosphor [5], waveguide films [6], and it was applied to stabilize the tetragonal phase of ZrO_2 [7] and to improve the densification of sintered SiC [8]. Recently, attempts are being made to use strongly paramagnetic Gd_2O_3 nanoparticles for contrast enhancement in magnetic resonance imaging (MRI) [9,10]. Furthermore, the possibility

of application of ultra-fineGd_2O_3nanoparticles to image brain cancer cells in vivo by MRI has been reported [11].

Generally, metal oxide nanoparticles can be prepared by thermal decomposition, co-precipitation, hydrothermal and solvothermal methods [12-14]. In the case of Gd_2O_3nanoparticles preparation, several methods including hydrothermal [9,10], combustion [15], sol-gel [16] and chemical reduction [17] have been applied until now. In liquid based synthesis methods, it is usually required to careful control of reaction parameters such as pH, temperature, and concentration of reactants for achieving the desired particle size and dispersion. Although, these methods have been improved in the recent years, however, control of the particle size and its distribution are still the challenges. For example, it is difficult to control product formation process in the chemical routes (like solvothermal and hydrothermal) which yield nanoparticles with a broad size distribution, irregular morphology and aggregated nature. Thus, it remains a challenge to develop a simple route to synthesize Gd_2O_3 nanoparticles with controlled size and shape in aqueous media. In this regard, electrochemical procedure i.e. cathodic electrodeposition can be an attractive technique for the synthesis of nanostructured Gd_2O_3 due to its powerful control on the structural and properties of products. In this technique, hydroxide of metal, as a precursor, is prepared by cathodic electrodeposition and then it convert to metal oxide by heat– treatment process [18,19]. In this work, we report, for the first time, preparation of Gd_2O_3 nanoparticles via pulse current electrodeposition followed by heat-treatment. The prepared nanoparticles were characterized by XRD, IR, TG, SEM and TEM techniques. To the best of our knowledge, preparation of Gd_2O_3 nanoparticles via this route has not been reported until now.

2. Experimental
2.1. Materials

$Gd(NO_3)_3 \cdot 6H_2O$ (Merck), graphite plates (TENNRY, China) and stainless steel sheets (TISCO, China) were purchased and used. All chemicals were of analytical grade and used without further purification. All solutions were prepared by using double distilled water. Aqueous solution of 5 mM $Gd(NO_3)_3 \cdot 6H_2O$ was prepared for electrodeposition.

2.2. Preparation of Gd_2O_3 nanoparticles

Gd_2O_3 nanoparticles were prepared by a two-step method. First, gadolinium hydroxide was electrodeposited in a two-electrode electrochemical cell system. The electrochemical cell included a stainless steel cathode (316L, 1cm × 0.5cm × 0.005cm) centered between two parallel graphite counter electrodes. Prior to each deposition, the steel substrates were galvanostatically electropolished at a current density of 0.5 A cm^{-2} for 5 min in a bath (70 $^{\circ}$C) containing 50 vol.% phosphoric acid, 25 vol.% sulfuric acid and balanced deionized water. The electrodeposition experiments were performed in a pulse current (PC) mode with applying the peak current density of 2mA cm^{-2} and at room temperature. The PC deposition was conducted at a typical on-time and off-time (t_{on}=1ms and t_{off}=1ms) for 60 min. For comparison, the electrodeposition experiments were also performed at direct current (2 mA cm^{-2}) with applying the same electrochemical conditions. After electrodeposition, the steel electrodes were rinsed with deionized water several times and dried at RT for 48h. Then the deposits were scraped from the steel electrodes and calcined at 600 $^{\circ}$C for 3h in dry air atmosphere to obtain oxide product.

2.3. Characterization methods

The crystal structure of the prepared sample was determined by powder X-ray diffraction (XRD) method using a Phillips PW-1800 diffractometer with Cu Kα radiation (λ=1.5406 Å) at a scanning rate of 1 degree/min. Thermal behavior analysis (TGA) were carried out in dry air atmosphere between room temperature and 600 $^{\circ}$C at a heating rate of 5 $^{\circ}$C min^{-1} using a thermoanalyzer (STA-1500). Chemical bonding information on metal–oxygen, metal–anions, and hydroxyl were studied with Fourier transform infrared spectroscopy (FTIR, Bruker Vector 22) using a potassium bromide (KBr) pellet technique. FTIR spectra were collected after 20 scans at a resolution of 4 cm^{-1} from 400 to 4000 cm^{-1}.The morphology of the samples was observed using a scanning electron microscope (SEM, LEO 1455 VP, Oxford, UK, operating voltage 30 kV) by mounting a small amount of the prepared powders on a conducting carbon tape and sputter coating with Pt to improve the conductivity. Transmission electron microscopy (TEM) images were also acquired using a Phillips EM 208 transmission electron microscope with an accelerating voltage of 100 kV.

3. Results and discussion

3.1. Crystal structure

Fig. 1 depicts the XRD patterns of the electrodeposited hydroxide precursor and the heat-treated final product. The positions the XRD peaks in Fig. 1a are similar to the lanthanide hydroxynitrate reported in the literature [20-22]. In fact, the XRD pattern of our electrodeposited hydroxide can be assigned to the composition of $Gd(OH)_2 NO_3 nH_2O$. The position and relative intensity of all diffraction peaks in Fig. 1b are also fully matched with the standard card of the cubic Gd_2O_3 phase (JCPDS card 88-2165). No diffraction peaks deal with any impurities like hydroxide precursor was observed indicating the complete conversion of gadolinium hydroxynitrate deposit to Gd_2O_3 during the calcination at 600 ℃ for 3h. The average crystallite size (D) was also calculated from the diffraction line-width of XRD patterns, based on Scherrer's relation (D=0.9λ/β cos (θ)), where, β is the full width at half maxima (FWHM) of the XRD peak. Notably, the diffraction peaks of (001) and (222) were used to obtain crystal size of deposited hydroxide and oxide samples, respectively. The calculations revealed that hydroxide and oxide samples have sizes of 13.4 and 18.5 nm, respectively.

3.2. FT-IR spectra

Fig. 2 contains the IR spectra of the prepared hydroxide and oxide samples. In both IR spectra, the broad peak located at 3400-3500 cm^{-1} is ascribed to stretching vibration of the hydroxyl groups connected to nanoparticle surface and also the adsorbed water [9]. Also, the bands at 1630-1640 cm^{-1} are related

to O–H deformation vibrations. It was reported that the band at approximately 1370-90 cm^{-1} is related to the presence of the nitrate anions in the interlayer position of the composition and indicative of an uncoordinated nitrate anion [21-23]. In addition, it has been also stated that due to the carbonate contamination in these materials it is necessary to use the presence of additional bands at ~1050 and ~1760 cm^{-1} to confirm the presence of the nitrate anion in the prepared compound. The latter is a typical vibration mode of nitrate and the former the v_1 mode which is observed as a result of the reduction in symmetry due to the intercalated form. For our deposited sample, a strong absorption peak at 1381 cm^{-1} and a broad one at 1052 cm^{-1} (Fig. 2a) are observed, which can be assigned to the vibration modes of NO_3^- anions inserted to the deposit during the electrodeposition process [15,16, 22]. It is worth noting that there is no any peak at 1760 cm^{-1}, which implicated that the nitrate ions in our deposit are mainly exist in the interlayer space of deposit structure with formula of $Gd(OH)_2NO_3H_2O$. In Ref. [22], it was stated that the presence of strong peak at approximately 1370 cm^{-1}, which is characteristic of an uncoordinated nitrate anion, supports that the nitrate is located between the lanthanide hydroxy layers rather than coordinated to the lanthanide cations, and clearly observed in the case of $La(OH)_2NO_3H_2O$ [24]. The peaks related to the nitrate are not observed in the IR spectral of Gd_2O_3 (Fig. 2b), indicates the removal of the intercalated nitrate ions during the heat-treatment process in agreement with DSC-TGA results. In both spectra, the peaks at about 1520, 1470 and 875 cm^{-1} in both samples can be attributed
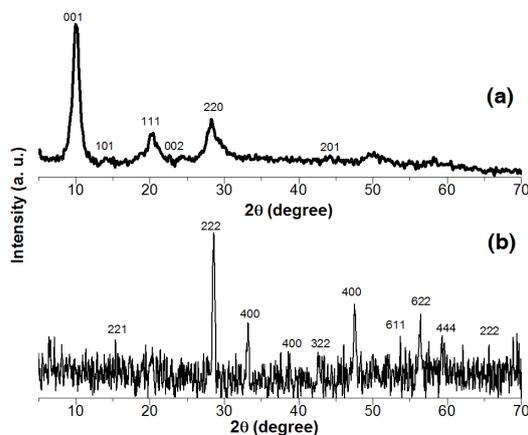

Fig. 1- XRD patterns of the prepared (a) $Gd(OH)_3$ and (b) Gd_2O_3 nanoparticles.
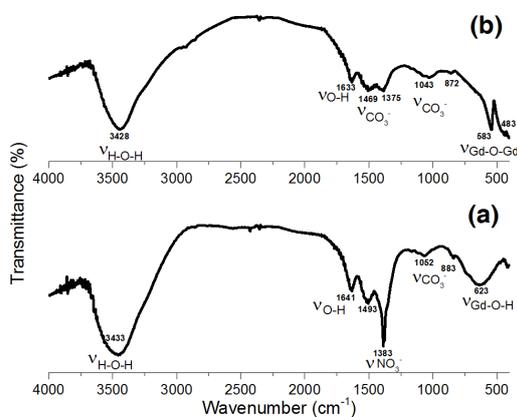

Fig. 2- IR spectra of the prepared $Gd(OH)_3$ and (b) Gd_2O_3 nanoparticles.

to the symmetric and asymmetric stretching vibrations of carbonate group, which may originate from air [20]. In Fig. 2a, the broad peak at 623 cm^{-1} is originated from the O–H bending of Gd–O–H [11]. For Gd_2O_3 (Fig. 2b), no OH vibration modes were observed as expected. The IR bands centered at about 583 cm^{-1} and 483 cm^{-1} can be assigned to the Gd-O vibrations of cubic Gd_2O_3 [21,25], which confirmed the oxide composition of the prepared product and is in agreement with the XRD results (Fig. 1b).

3.3. Morphology

Morphological characteristics of the prepared samples were determined by SEM and TEM observations. The SEM images of the prepared samples are shown in Fig. 3. Both hydroxide and oxide samples have particle morphology and no obvious aggregation is observed. The prepared samples (i.e. hydroxide and oxide) have smooth surface and completely spherical particles with good dispersions as seen in Figs. 3a and b. However, due to the ultrafine size of both samples particles,

more information could not be detected from the SEM images. Fig. 4 shows the TEM images of hydroxide deposit and Gd_2O_3 particles. High magnification by TEM revealed that both samples are composed of well–dispersed ultrafine particles with the uniform size (Fig. 4). From the TEM images, the mean size of the prepared hydroxide deposit and Gd_2O_3 nanoparticles were measured to be 15 and 20 nm, respectively. These observations are completely in agreement with the calculated crystallite sizes from XRD patterns of both samples (Fig. 1). The morphology of the prepared samples by DC electrodeposition are also evaluated by SEM and shown in Fig. 5. The deposited hydroxide has composed of sphere-like morphology at nanoscale (Fig. 5a). For the oxide sample, approximately the same sphere morphology is also seen. The size distributions of the prepared spheres are not uniform where they have diameters in the range of 100-200 nm, and rather agglomerated. In the SEM images of both DC deposited hydroxide and final oxide samples, there are the small particles in addition to the mentioned spheres, while the
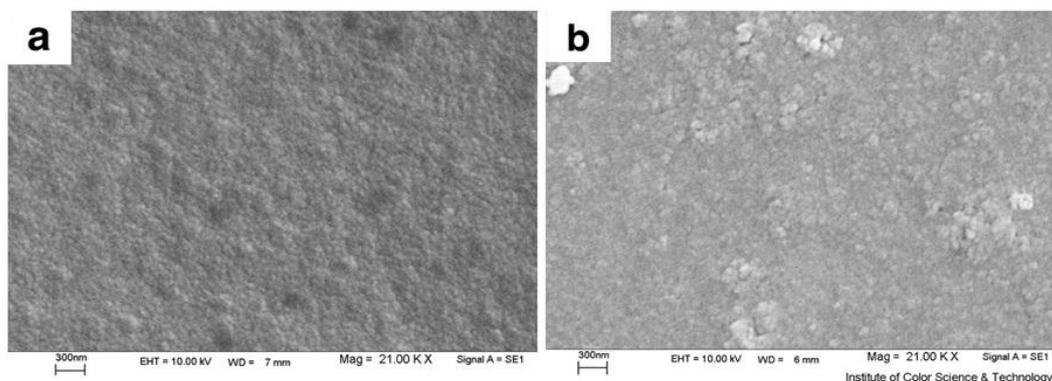

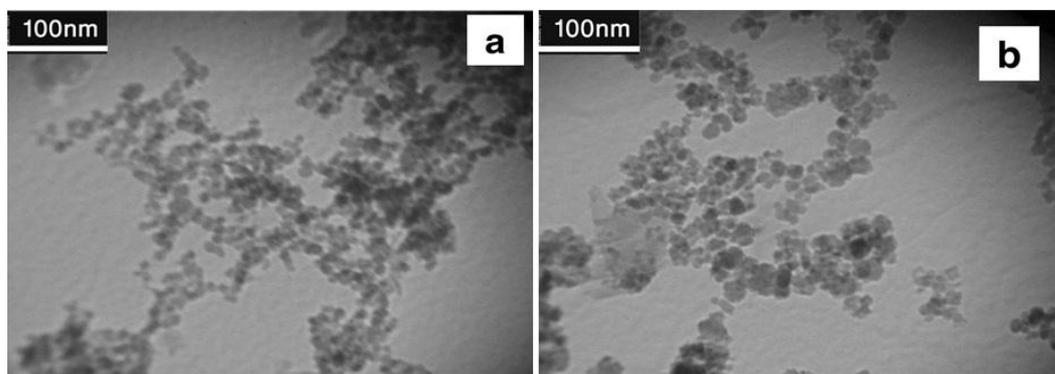Fig. 3- SEM images of the prepared (a) Gd(OH)$_3$ and (b) Gd$_2$O$_3$ nanoparticles.

Fig. 4- TEM images of the prepared (a) Gd(OH)$_3$ and (b) Gd$_2$O$_3$ nanoparticles.
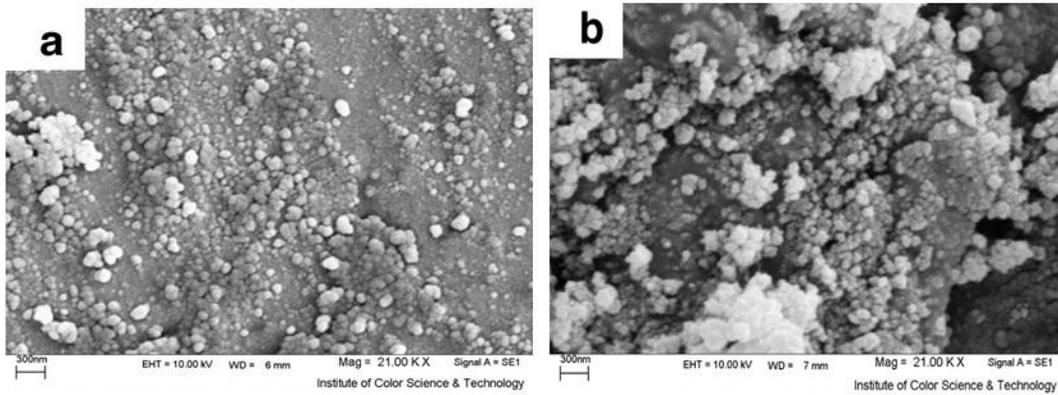
Fig. 5- Schematic view of the electrochemical formation of Gd(OH)$_3$ nanoparticles.
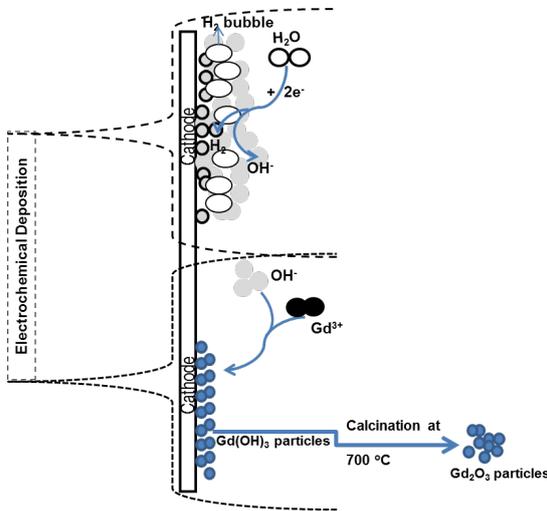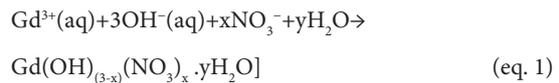

Fig. 6- (a) DSC and (b) related TG curves of the Gd(OH)$_3$ nanoparticles.

prepared sample by PC deposition are composed of well–dispersed ultrafine particles with the uniform size (Figs. 3 and 4).

3.4. Mechanism of Gd(OH)$_3$ deposition

A schematic illustration of the electrochemical deposition steps is shown in Fig. 6. Formation of the Gd(OH)$_3$ deposit on the cathode surface is occurred via a two–step electrochemical–chemical (EC) mechanism [18,19]. In this work, the electrodeposition experiments were performed in the pulse current regime, applying I$_p$ of 2 mA cm^{-2}. Considering the potential value of cathode (-0.92 V vs. Ag/AgCl), it is expected that the reduction of water molecules reduction reaction (i.e. $2H_2O + 2e^- \rightarrow H_2 + 2OH^-$) has a major role in the electrogeneration of base (OH$^-$) at the applied

current density as shown in Fig. 6. By increasing the OH$^-$ concentration to the required conditions, gadolinium hydroxide is formed and deposited on the cathode in the chemical step, as follow;

$$Gd^{3+}(aq)+3OH^-(aq)+xNO_3^-+yH_2O\rightarrow$$

$$Gd(OH)_{(3-x)}(NO_3)_x \cdot yH_2O] \qquad (eq. 1)$$

3.5. Gd$_2$O$_3$ formation mechanism

Thermal behavior of hydroxide precursor and its conversion to oxide during heat-treatment was evaluated using thermogravimetric method. The DSC and related TG curve of the hydroxide deposit particles are shown in Fig. 7. The DSC curve in Fig. 7a indicates three endothermic peaks at the interval of 25-150°C, 150-330°C and 330-600°C. Notably, the observed thermal behavior for our sample is similar to the reported ones for lanthanum hydroxynitrate (i.e. Ln(OH)$_2$(NO$_3$) .yH$_2$O; Ln= La, Y, Gd, Lu, Er,...) [21-23,26]. Hence, the chemical formula of Gd(OH)$_2$(NO$_3$) .yH$_2$O can be estimated for the deposited hydroxide. In addition to DSC, TG curve have three distinct and significant weight losses. In the first interval, below 150°C, DSC curve shows a broad endothermic peak, which is corresponds to removal of physically adsorbed H$_2$O on the nanoparticles:

$$[Gd(OH)_{2.5}(NO_3)_{0.5} \cdot yH_2O] \rightarrow [Gd(OH)_{2.5}(NO_3)_{0.5}] + yH_2O \quad (eq. 2)$$

For this step, the weight loss of 10.1% is observed from the TG curve (Fig. 7b). From this weight loss, one can easily estimate the value of physically adsorbed water on the nanoparticle surface. Our calculations give y=1.5 for the deposited hydroxide. Considering the y value in Eq. (2), the theoretical value of weight loss is determined to be about
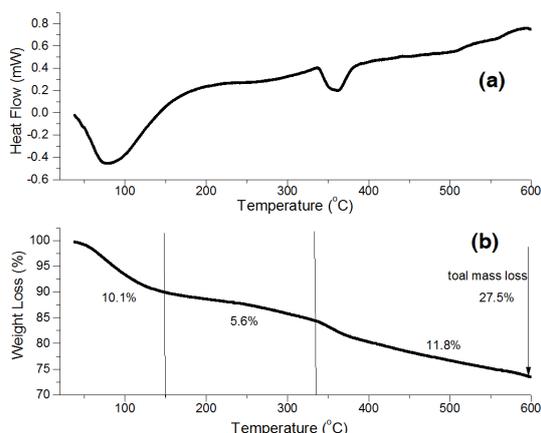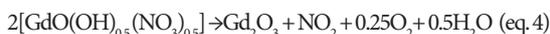
Fig. 7- (a) DSC and (b) related TG curves of the deposited hydroxide.

10.49%, which is close to the observed in the TG curve (i.e. 10.1%)

On DCS curve, the second broad and small endothermic peak at 150-330°C is related to the removal of structural water:

$$[Gd(OH)_{2.5}(NO_3)_{0.5}] \rightarrow [GdO(OH)_{0.5}(NO_3)_{0.5}] + H_2O \quad (eq. 3)$$

For this step, 5.6% weigh loss is observed on the TG curve. The last interval on the DCS curve, between 330 and 600°C, has a broad endothermic peak and can be assigned to the removal of the residual structural water and nitrate ions from $GdO(OH)_{0.5}(NO_3)_{0.5}$ [12,21,22]:

$$2[GdO(OH)_{0.5}(NO_3)_{0.5}] \rightarrow Gd_2O_3 + NO_2 + 0.25O_2 + 0.5H_2O \quad (eq. 4)$$

For this stage, the TG curve exhibits weigh loss of 11.8%. Total weight loss of the deposited sample is 27.5 wt.%, as could be seen from TG curve (Fig. 7b). Approximately 10.1 wt.% of the total amount of weight loss corresponds to physically adsorbed water. Also, the weight loss of 17.4 wt.% is related to removal of the structural water and nitrate ions.

4. Conclusion

Gd(OH)$_3$ nanoparticles were successfully deposited by pulse cathodic electrodeposition from gadolinium nitrate bath at mild condition. Gd$_2$O$_3$ nanoparticles were then obtained by the thermal annealing of Gd(OH)$_3$ at 600°C. The SEM and TEM observations revealed that heat treatment has no effect on the morphology of the hydroxide precursor. The XRD and IR results confirmed the characteristics of gadolinium hydroxynitrate (i.e. Gd(OH)$_{2.5}$(NO$_3$)$_{0.5}$ 1.5H$_2$O) and cubic Gd$_2$O$_3$ crystalline phases for the prepared samples before and after thermal annealing, respectively.

Mechanism of the oxide formation during calcination was clarified by DSC-TG analysis. Finally, it was concluded that pulse cathodic electrodeposition followed by heat-treatment opens new route to the preparation of Gd$_2$O$_3$ nanoparticles.

References:

1. Beek WJ, Wienk MM, Janssen RA. Efficient hybrid solar cells from zinc oxide nanoparticles and a conjugated polymer. Advanced Materials. 2004;16(12):1009-13.

2. Oskam G. Metal oxide nanoparticles: synthesis, characterization and application. Journal of Sol-Gel Science and Technology. 2006;37(3):161-4.

3. Tsuzuki T, Pirault E, McCormick PG. Mechanochemical synthesis of gadolinium oxide nanoparticles. Nanostructured Materials. 1999;11(1):125-31.

4. Colussi S, de Leitenburg C, Dolcetti G, Trovarelli A. The role of rare earth oxides as promoters and stabilizers in combustion catalysts. Journal of Alloys and Compounds. 2004;374(1):387-92.

5. Chang C, Kimura F, Kimura T, Wada H. Preparation and characterization of rod-like Eu: Gd$_2$O$_3$ phosphor through a hydrothermal routine. Materials Letters. 2005;59(8):1037-41.

6. Garcıa-Murillo A, Le Luyer C, Garapon C, Dujardin C, Bernstein E, Pedrini C, Mugnier J. Optical properties of europium-doped Gd$_2$O$_3$ waveguiding thin films prepared by the sol–gel method. Optical Materials. 2002;19(1):161-8.

7. Bhattacharyya S, Agrawal DC. Preparation of tetragonal ZrO$_2$- Gd$_2$O$_3$ powders. Journal of Materials Science. 1995;30(6):1495-9.

8. Chen Z. Effects of gadolinia and alumina addition on the densification and toughening of silicon carbide. Journal of the American Ceramic Society. 1996;79(2):530-2.

9. Babić-Stojić B, Jokanović V, Milivojević D, Požek M, Jagličić Z, Makovec D, Arsikin K, Paunović V. Gd$_2$O$_3$ nanoparticles stabilized by hydrothermally modified dextrose for positive contrast magnetic resonance imaging. Journal of Magnetism and Magnetic Materials. 2016;403:118-26.

10. Fang J, Chandrasekharan P, Liu XL, Yang Y, Lv YB, Yang CT, Ding J. Manipulating the surface coating of ultra-small Gd$_2$O$_3$ nanoparticles for improved T 1-weighted MR imaging. Biomaterials. 2014;35(5):1636-42.

11. Faucher L, Guay-Bégin AA, Lagueux J, Côté MF, Petitclerc É, Fortin MA. Ultra-small gadolinium oxide nanoparticles to image brain cancer cells in vivo with MRI. Contrast Media & Molecular Imaging. 2011;6(4):209-18.

12. Dehno Khalaji A. Nickel Oxide (NiO) nanoparticles prepared by solid-state thermal decomposition of Nickel (II) schiff base precursor. Journal of Ultrafine Grained and Nanostructured Materials. 2015;48(1):1-4.

13. Farahmandjou M, Zarinkamar M. Synthesis of nano-sized ceria (CeO$_2$) particles via a cerium hydroxy carbonate precursor and the effect of reaction temperature on particle morphology. Journal of Ultrafine Grained and Nanostructured Materials. 2015;48(1):5-10.

14. Khadivi Ayask H, Vahdati Khaki J, Haddad Sabzevar M. Facile synthesis of copper oxide nanoparticles using copper hydroxide by mechanochemical process. Journal of Ultrafine Grained and Nanostructured Materials. 2015;48(1):37-44.

15. Dhananjaya N, Nagabhushana H, Nagabhushana BM, Rudraswamy B, Sharma SC, Sunitha DV, Shivakumara C, Chakradhar RP. Effect of different fuels on structural, thermo

and photoluminescent properties of Gd_2O_3 nanoparticles. Spectrochimica Acta Part A: Molecular and Biomolecular Spectroscopy. 2012;96:532-40.

16. Rahman AA, Vasilev K, Majewski P. Ultra small Gd_2O_3 nanoparticles: absorption and emission properties. Journal of Colloid and Interface Science. 2011;354(2):592-6.

17. Yang S, Gao H, Wang Y, Xin S, He Y, Wang Y, Zeng W. A simple way to synthesize well-dispersed Gd_2O_3 nanoparticles onto reduced graphene oxide sheets. Materials Research Bulletin. 2013;48(1):37-40.

18. Abed F, Aghazadeh M, Arhami B. Preparation of Gd_2O_3 coral-like nanostructures by pulse electrodeposition–heat-treatment method. Materials Letters. 2013;99:11-3.

19. Aghazadeh M, Yousefi T. Preparation of Gd_2O_3 nanorods by electrodeposition–heat-treatment method. Materials Letters. 2012;73:176-8.

20. Poudret L, Prior TJ, McIntyre LJ, Fogg AM. Synthesis and crystal structures of new lanthanide hydroxyhalide anion exchange materials, $Ln_2(OH)_5X·1.5H_2O$(X= Cl, Br; Ln= Y, Dy, Er, Yb). Chemistry of Materials. 2008;20(24):7447-53.

21. Hindocha SA, McIntyre LJ, Fogg AM. Precipitation synthesis of lanthanide hydroxynitrate anion exchange materials, $Ln_2(OH)_5NO_3· H_2O$ (Ln= Y, Eu–Er). Journal of Solid State Chemistry. 2009;182(5):1070-4.

22. McIntyre LJ, Jackson LK, Fogg AM. $Ln_2(OH)_5NO_3·xH_2O$(Ln= Y, Gd– Lu): A Novel Family of Anion Exchange Intercalation Hosts. Chemistry of Materials. 2007;20(1):335-40.

23. Fogg AM, Williams GR, Chester R, O'Hare D. A novel family of layered double hydroxides—$[MAl_4(OH)_{12}](NO_3)_2$ $.xH_2O$ (M= Co, Ni, Cu, Zn). Journal of Materials Chemistry. 2004;14(15):2369-71.

24. Louett M, Louer D. The structures of lanthanum hydroxide nitrates investigated by the Rietveltl profile refinement technique. European Journal of Solid State Inorganic Chemistry. 1989;26:241.

25. Kang JG, Min BK, Sohn Y. Synthesis and characterization of $Gd(OH)_3$ and Gd_2O_3 nanorods. Ceramics International. 2015;41(1):1243-8.

26. Schildermans I, Mullens J, Van der Veken BJ, Yperman J, Franco D, Van Poucke LC. Preparation and thermal decomposition of $Cu_2(OH)_3NO_3$. Thermochimica Acta. 1993;224:227-32.